

# Recent results on light hadron and quark masses

R.D. Kenway<sup>a</sup>

<sup>a</sup>Department of Physics and Astronomy, The University of Edinburgh,  
The King's Buildings, Edinburgh EH9 3JZ, Scotland

Recent results for the spectrum of light hadrons provide clear evidence for the failure of quenched QCD and encouraging signs that simulations with dynamical sea quarks rectify some of the discrepancies, although string breaking has not yet been observed. The use of perturbation theory to match lattice quark masses to continuum schemes remains questionable, but non-perturbative methods are poised to remove this uncertainty. The inclusion of dynamical sea quarks substantially reduces estimates of the light quark masses. New results for the lightest glueball and the lightest exotic hybrid state provide useful input to phenomenology, but still have limited or no treatment of mixing. The  $O(a)$ -improved Wilson quark action is well-established in quenched QCD for  $\beta \geq 5.7$ , with most parameters obtainable non-perturbatively, in which range scaling violations are small. Progress has also been made with high-order improvement schemes for both Wilson and staggered quarks.

## 1. INTRODUCTION

Calculation of the light hadron spectrum is an essential part of any numerical simulation of QCD, because it provides the most direct way of fixing the quark masses. The bare mass for each quark flavour is tuned until the masses of correspondingly flavoured hadrons agree with experiment, having chosen one dimensionful quantity to set the overall scale. It is expensive to simulate at masses much below that of the strange quark, so the  $u$  and  $d$  quark masses must be obtained by chiral extrapolation. Electromagnetic corrections are ignored, so we cannot distinguish the  $u$  and  $d$  masses.

The hadron spectrum is widely used to test scaling for improved lattice actions; the improvement programme being our best hope for reliable simulations with dynamical sea quarks. Once the known hadron masses have been used to validate the simulations, the spectrum calculations provide important predictions for phenomenology. They are guiding searches for glueballs and for exotic mesons. Finally, the light quark masses are some of the poorest-known Standard Model parameters and these uncertainties matter; for instance, Standard Model predictions of  $\epsilon'/\epsilon$  are very sensitive to  $m_s + m_d$  [1]. The challenge is to find a reliable way of matching the lattice

quark masses to those in a continuum perturbative scheme, which can be used for phenomenology.

### 1.1. The determination of quark masses

Quarks do not appear as asymptotic states in QCD, because of confinement. As a consequence, it is usual to quote values for the running quark mass at a particular scale in a specific scheme, eg  $m^{\overline{\text{MS}}}(2 \text{ GeV})$ , although, alternatively, we could run the mass up to high scales and quote the RG invariant (scheme independent) value

$$M = \lim_{\mu \rightarrow \infty} m (2b_0 g^2)^{-d_0/2b_0} \quad (1)$$

where

$$\mu \frac{\partial g}{\partial \mu} = \beta(g) = -b_0 g^3 + \dots \quad (2)$$

$$\mu \frac{\partial m}{\partial \mu} = \tau(g) m = -d_0 g^2 m + \dots \quad (3)$$

Given  $M$ , it is straightforward to run the mass down to any desired scale, using continuum perturbation theory, provided we remain within the perturbative regime.

For Wilson quarks, the pseudoscalar meson mass vanishes at  $\kappa = \kappa_{\text{crit}}$  and the bare quark mass is

$$m_q a = \frac{1}{2\kappa_q} - \frac{1}{2\kappa_{\text{crit}}} \quad (4)$$

where  $\kappa_q$  is determined by tuning the mass of a  $q$ -flavoured hadron to its experimental value. The renormalised quark mass may be determined either using the vector Ward identity (conserved current),

$$\langle \partial_\mu V_\mu^a(x) \mathcal{O}(0) \rangle = \left[ \frac{1}{2\kappa_2} - \frac{1}{2\kappa_1} \right] \frac{\langle S^a(x) \mathcal{O}(0) \rangle(\mu)}{Z_S(\mu a)} \quad (5)$$

so that

$$m_q^{\overline{\text{MS}}}(\mu) = Z_S(\mu a)^{-1} m_q = Z_m(\mu a) m_q, \quad (6)$$

or the axial Ward identity,

$$(m_1 + m_2)(\mu) = \frac{Z_A}{Z_P(\mu a)} \frac{\langle \partial_\mu A_\mu^a(x) \mathcal{O}(0) \rangle}{\langle P^a(x) \mathcal{O}(0) \rangle(a)}, \quad (7)$$

which gives the renormalised quark masses without using  $\kappa_{\text{crit}}$ . Here, quantities denoted at the scale  $\mu$  ( $a$ ) are renormalised (bare). For staggered quarks, the remnant chiral symmetry ensures  $Z_A = 1$ ,  $Z_P = Z_S = Z_m^{-1}$ , so both methods are essentially the same (unfortunately, the 1-loop term in the matching is large, casting doubt on the reliability of perturbation theory).

## 1.2. Some important questions

In reviewing recent results for the light hadron spectrum, I will focus on the following questions. Can we conclude that quenched QCD is wrong? To what extent have we observed effects which can be attributed to dynamical sea quarks? How effective are improved actions at reducing scaling violations? Is the matching of lattice and continuum quark masses under control? Finally, I will report on a few phenomenologically important predictions for glueballs and hybrids.

## 2. QUENCHED APPROXIMATION

It has been known for some time that the quenched approximation gets the spectrum in the strange sector wrong and underestimates hyperfine splittings [2]. There are several related symptoms of this failure, in particular, using  $M_K$  and  $M_\phi$  as input gives different values for the strange quark mass.

### 2.1. Chiral extrapolations

Chiral extrapolation is now the main source of systematic error and a key issue is whether

the data requires the inclusion of quenched chiral logarithms. If so, we need to be able to control the extrapolation to within a few percent to show that the quenched approximation breaks down in the  $ud$  sector too. CP-PACS has reported such results for the Wilson quark action at this conference, having increased the statistics at its smallest lattice spacing during the year [3,4]. As yet, though, this failure of the quenched approximation has not been confirmed using staggered quarks, or other improved actions.

In quenched QCD, the  $\eta'$  meson remains light in the chiral limit, because the infinite series of loop diagrams, which gives it a non-zero mass in the full theory, is absent [5]. The singlet 2-point function has a double pole, giving rise to so-called quenched chiral logarithms, which diverge as  $m_q \rightarrow 0$ . The renormalisation of quenched chiral perturbation theory has been carried out at one loop [6]. Anomalous chiral behaviour persists in dynamical simulations when the valence-quark and sea-quark masses are different, as is necessarily the case for the strange quark in simulations with  $N_f = 2$  sea quarks (partial quenching), and this can produce strong dependence on the sea-quark mass when both it and the valence-quark mass are small [7].

The CP-PACS data are consistent with the presence of quenched chiral logarithms [3,4]. Both the pseudoscalar meson masses and decay constants indicate a non-zero value for the coefficient of the leading quenched chiral logarithm,  $\delta = 0.10(2)$ . Also, using quenched chiral perturbation theory to extrapolate the pseudoscalar meson mass to zero, gives a value of  $\kappa_{\text{crit}}$  in better agreement with a linear extrapolation of the axial Ward identity quark mass, than a simple quadratic polynomial in the quark mass.

### 2.2. The quenched QCD spectrum

The evidence of a non-zero value for  $\delta$  justifies CP-PACS's use of quenched chiral perturbation theory to produce their final results for the quenched spectrum. They obtain the continuum limit, shown in Fig 1, by linearly extrapolating data at four lattice spacings, with  $a^{-1}$  ranging from 2 to 4 GeV, on lattices which are all roughly 3 fm in size.

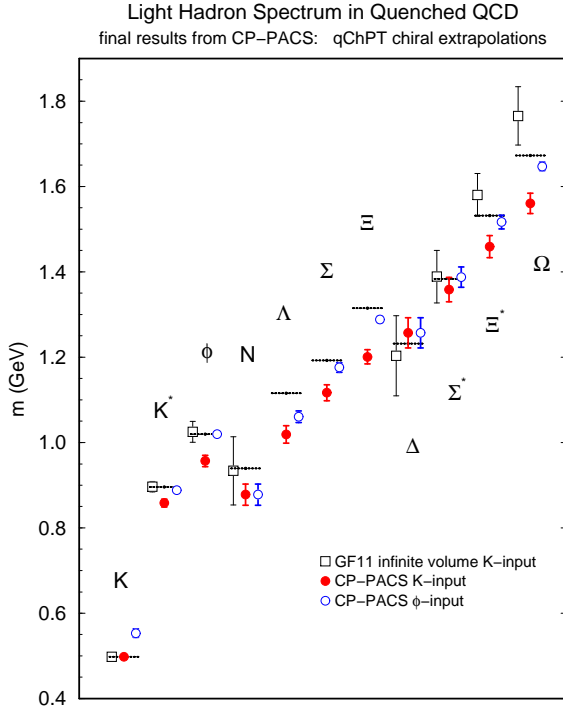


Figure 1. CP-PACS results for the light hadron spectrum in quenched QCD obtained using the Wilson quark action [3,4].

Fig 1 confirms the picture that there is no choice for the strange quark mass which can explain the whole spectrum. Using  $M_K$  as input, the meson hyperfine splitting, the octet baryon masses, and the decuplet baryon mass splittings, are all too small. Using  $M_\phi$  to fix the strange quark mass reduces the discrepancies amongst the baryon masses, but the other faults remain. The problem is not due to the way in which the strange quark mass is defined; as can be seen in Fig 2, the vector and axial Ward identity definitions agree in the continuum limit, but with limiting values which depend on the choice of input:

$$m_s^{\overline{\text{MS}}}(2 \text{ GeV}) = \begin{cases} 143(6) \text{ MeV} & (M_\phi \text{ input}) \\ 115(2) \text{ MeV} & (M_K \text{ input}) \end{cases} \quad (8)$$

The CP-PACS result for the  $u$  and  $d$  quark mass is

$$m_{ud}^{\overline{\text{MS}}}(2 \text{ GeV}) = 4.55(18) \text{ MeV} \quad (9)$$

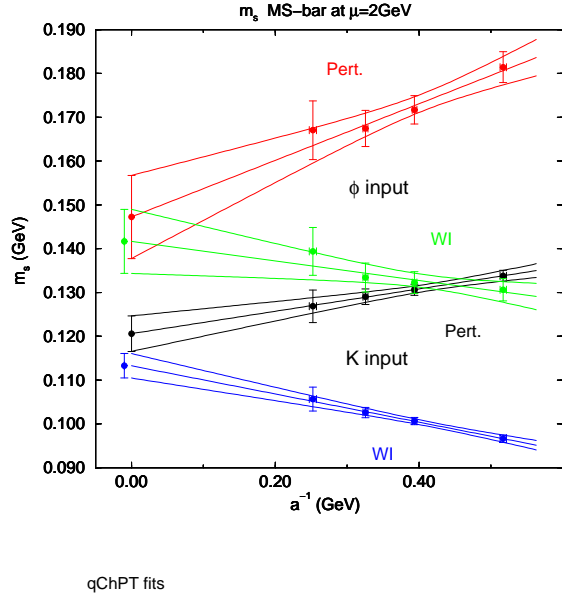


Figure 2. CP-PACS results for the strange quark mass in quenched QCD, defined using the vector (Pert in the figure) and axial (WI) Ward identities [3,4].

again with consistency between the two definitions in the continuum limit. The problem with the strange quark mass is directly related to the low value of  $J \equiv M_{K^*}(dm_V/dm_{\text{PS}}^2)$ , since

$$\frac{(m_s)_K}{(m_s)_\phi} = \left[ \left( \frac{M_{K^*}}{M_K} \right)^2 \left( 1 + \frac{m_{ud}}{m_s} \right) \right]^{-1} \frac{2J}{\frac{M_\phi}{M_{K^*}} - \frac{m_V(0)}{M_{K^*}}} \quad (10)$$

if linear chiral behaviour is assumed for  $m_{\text{PS}}^2$  and  $m_V$  [8].

It is desirable to confirm the CP-PACS results using an improved action. The most direct comparison of this sort is with MILC results [9,10] for staggered quarks, which are also available on lattices of at least 3 fm in size. Chiral extrapolation again turns out to be the most delicate issue. For staggered quarks, it is the mass of the non-Goldstone pion which appears in quenched chiral perturbation theory, and MILC includes terms linear in this mass in the chiral extrapolation of the nucleon and vector meson masses. The continuum extrapolation is shown in Fig 3 and,

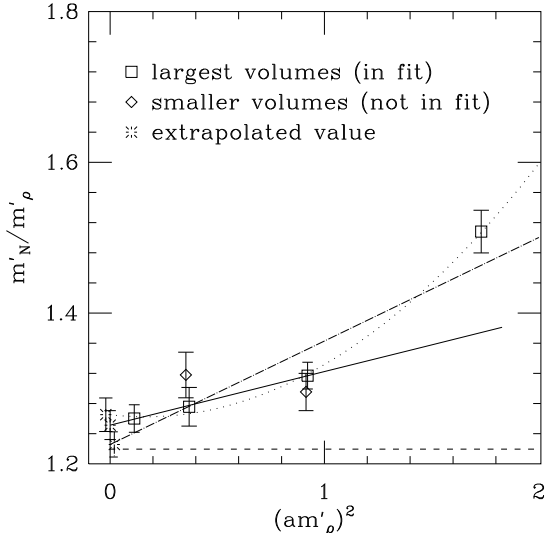


Figure 3. Continuum extrapolation of MILC data for  $m'_N/m'_\rho$  in quenched QCD, using staggered quarks [9,10].

combining various chiral and continuum fits, they quote the final result

$$\frac{m_N}{m_\rho} = 1.254 \pm 0.018 \pm 0.027, \quad (11)$$

in agreement with the experimental value of 1.22. The statistical error is similar to that of CP-PACS, and the difference between the results is only  $2.5\sigma$ , which is not a serious disagreement. It would be interesting to combine the MILC data with that of Kim and Ohta [11], which is on a similar size lattice, but with a smaller lattice spacing ( $\beta = 6.5$ ), to see if this error can be reduced.

In summary, CP-PACS has provided us with evidence of the breakdown of the quenched approximation for light hadrons at the few percent level, the most striking symptom of this being non-uniqueness of the strange quark mass, although confirmation from improved actions is still awaited.

### 3. SEA-QUARK EFFECTS

During the last few years, several groups have begun systematically to explore the parameter

space for simulations with dynamical quarks. Finite-size effects must be checked, and this is not as straightforward as in quenched QCD, because the lattice spacing at fixed sea-quark mass depends on the physical quantity used to define it, and decreases significantly with the sea-quark mass. So the volume is only well-defined for chiral sea quarks.

I will focus on simulations with two degenerate flavours of sea quark, which may represent  $u$  and  $d$ , in which case the strange quark must be treated in the quenched approximation. The data for Wilson quarks, obtained with unimproved and various choices of improved action (SESAM [12], CP-PACS [3,13] and UKQCD [14]), correspond to mass ratios  $m_{PS}/m_V$  between 0.6 and 0.8, and lattice sizes of around 2 fm, whereas the MILC data for staggered quarks [10] extend to a mass ratio of around 0.3 on lattices which are somewhat larger.

#### 3.1. Wilson quarks

UKQCD has explored finite-size effects for hadron masses, in which valence and sea-quark masses are the same, and finds that a significant effect occurs at the lower end of the above range of quark masses, between lattice sizes of 0.9 and 1.4 fm [14]. Above 1.4 fm, no effect is observed. Consequently, chiral extrapolations using linear and quadratic polynomials in the valence and sea-quark masses, and including cross-terms, is probably safe for the Wilson quark data mentioned above.

SESAM notes that data at different sea-quark masses are uncorrelated, so that the error in the chiral extrapolation is larger than for quenched QCD, probably obscuring sea-quark effects [12]. As reported by CP-PACS [3,13], the trend in the light hadron masses, as lattice spacing decreases, is to agree with experiment, but the statistical errors are still large compared to the quenched QCD results, where the discrepancy with experiment is small anyway, and CP-PACS does not attempt a continuum extrapolation.

#### 3.2. Staggered quarks

The results obtained by MILC for  $N_f = 2$  staggered quarks [10] are perhaps the most surpris-

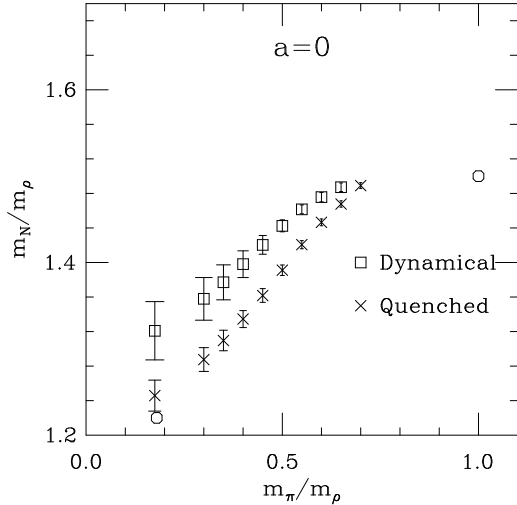


Figure 4. Edinburgh plot comparing continuum results for quenched and  $N_f = 2$  QCD using staggered quarks, obtained by MILC [10].

ing at this year's conference. They perform a  $\text{const} + O(a^2)$  continuum extrapolation of data at five lattice spacings, at fixed  $m_\pi/m_\rho$ , to produce the Edinburgh plot shown in Fig 4. Although the continuum and chiral extrapolations appear to be well behaved, the dynamical results lie systematically above the quenched results, and so deviate further from experiment. This is true even at large quark masses, where the entire calculation should be under control!

### 3.3. The strange-quark sector

Returning to the Wilson data, we might hope to see an improvement in the strange sector from dynamical quarks. CP-PACS reports a tendency for the strange meson splitting to increase as the continuum limit is approached [3,13], in better agreement with experiment than the quenched data, as shown in Fig 5.

SESAM points out that  $J$  no longer has a simple interpretation as the slope of the vector meson mass with respect to the square of the pseudoscalar meson mass,  $m_{PS}$ , because  $J$  is no longer

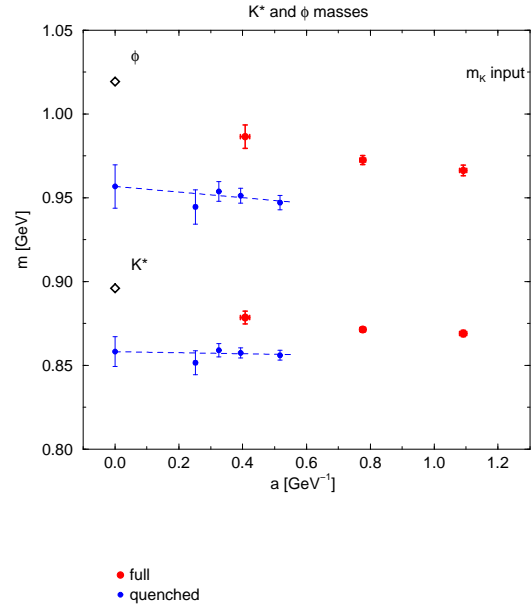


Figure 5. Comparison of the strange meson splitting in quenched and  $N_f = 2$  QCD, obtained by CP-PACS [3,13].

a function only of  $m_{PS}$ , but depends separately on the valence and sea-quark masses [12]. Thus, chiral extrapolation cannot be avoided in computing  $J$ . At fixed sea-quark mass and fixed lattice spacing, there is no improvement in the value of  $J$  compared to the quenched approximation, and there is no discernable dependence on the sea-quark mass, as noted also by UKQCD [12,14]. This could be due to the continued use of the quenched approximation for the strange quark.

### 3.4. Quark masses

Partial quenching, in which the valence and sea-quark masses are taken to be different, and which is necessary for the strange quark in  $N_f = 2$  simulations, allows for an alternative definition of quark mass at non-zero lattice spacing. The partially-quenched quark mass is defined as

$$m^{\text{PQ}}a \equiv \left( \frac{1}{2\kappa_{\text{valence}}} - \frac{1}{2\kappa_{\text{crit}}(\kappa_{\text{sea}})} \right) \quad (12)$$

where  $\kappa_{\text{crit}}(\kappa_{\text{sea}})$  is defined by the vanishing of the pseudoscalar meson mass, at fixed  $\kappa_{\text{sea}}$ . Last

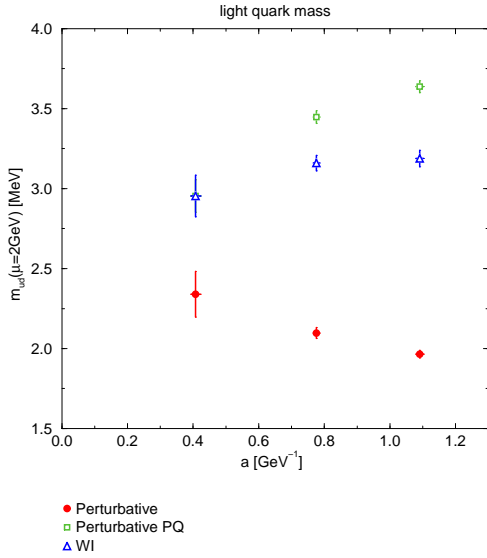


Figure 6. CP-PACS results for the  $ud$  quark mass in two-flavour QCD at three lattice spacings, using the vector WI (Perturbative in the figure), axial WI (WI) and partially-quenched (Perturbative PQ) definitions [3,13].

year, SESAM reported that  $\kappa_{\text{crit}}(\kappa_{\text{sea}})$  depends strongly on  $\kappa_{\text{sea}}$  [15].

CP-PACS takes  $\kappa_{\text{sea}} = \kappa_{ud}$  to define a partially-quenched mass. Their results [3,13] in Fig 6 show that, at fixed lattice spacing, the partially-quenched, vector and axial Ward identity masses all disagree. However, it appears that, within the relatively large statistical errors, all definitions are converging to a continuum limit of around 2.5 MeV, although the data is not good enough to justify an extrapolation. As shown in Fig 7, CP-PACS also finds that the estimates for the strange quark mass, obtained using the  $K$  and  $\phi$  masses, disagree at non-zero lattice spacing, but, within the large statistical errors, appear to be consistent with a single continuum limit around 80 MeV. Evidently, there is a large quenching effect which overestimates the light quark masses by as much as 40%. It should be noted that the results for the strange quark mass may still be an overestimate due to the use of partial quenching. In fact, CP-PACS estimates

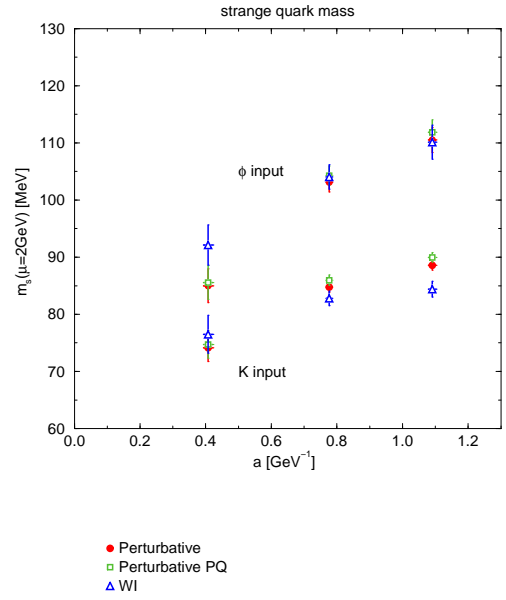


Figure 7. Comparison of CP-PACS results for the  $s$  quark mass, determined from the  $\phi$  and from the  $K$  meson masses, in two-flavour QCD [3,13].

for the ratio  $m_s/m_{ud}$  from the axial Ward identity are essentially independent of lattice spacing at a value of about 25 [3,13], consistent with lowest-order chiral perturbation theory, although a slightly smaller value is favoured at next order [16].

### 3.5. String breaking

The much-hoped-for signal of sea-quark effects is, of course, string-breaking. Although Philipsen and Wittig have demonstrated very clearly the crossover from a string-like to a two-meson state in a  $(2+1)$ -dimensional  $SU(2)$  Higgs model [17], zero-temperature QCD results, such as those from UKQCD in Fig 8, show little dependence of the potential at large distances on sea-quark mass [14]. It is likely that the Wilson loop operator does not project well onto broken string states outside a narrow mixing region [17], and a computation of the full matrix correlator of Wilson loops and two-meson operators is needed, but see [18] for further discussion of this.

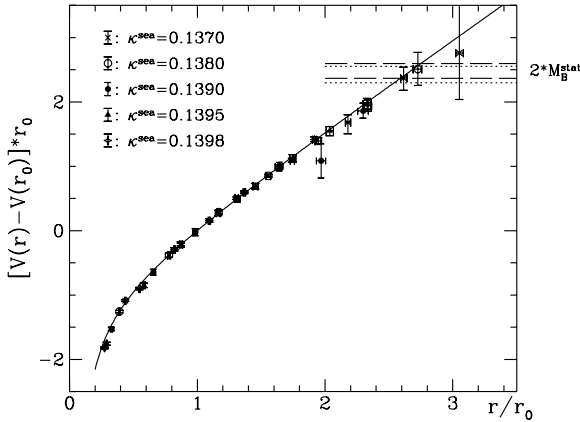


Figure 8. UKQCD results for the static quark potential in two-flavour QCD for different sea-quark masses [14].

#### 4. IMPROVED ACTIONS

Improvement at least to  $O(a)$  is necessary for dynamical quark simulations and considerable progress has been made in recent years, particularly by the Alpha Collaboration, in implementing this non-perturbatively for Wilson quarks. Most of the scaling tests have been performed in quenched QCD, but some dynamical results are now becoming available. Higher-order improvement has the potential for big pay-offs, but many parameters have to be fixed reliably.

##### 4.1. $O(a)$ -improved Wilson quarks

This requires one additional term in the action,

$$c_{\text{SW}} \frac{a^5}{4} \sum_x \bar{q}(x) i\sigma_{\mu\nu} F_{\mu\nu}(x) q(x), \quad (13)$$

as noted first by Sheikholeslami and Wohlert (SW), plus explicit determination of the mass dependence (coefficients  $b_A, \dots$ ) and mixing (coefficients  $c_A, \dots$ ) at  $O(a)$  of composite fields:

$$\mathcal{O}^{\text{R}} = Z_{\mathcal{O}}(1 + b_{\mathcal{O}} am_q)(\mathcal{O} + \sum_n c_n a \mathcal{O}_n). \quad (14)$$

Using Schrödinger functional methods at  $m_q = 0$ , Alpha has determined many of the coefficients for quenched QCD for  $\beta \geq 6.0$  ( $a \leq 0.1$  fm), by imposing chiral symmetry, which is broken at  $O(a)$

by the Wilson action (for a review see [19]). De Ditiis and Petronzio use the quark-mass dependence of the PCAC relation to extract  $b_A - b_P$ ,  $b_V - b_S$ ,  $b_m$ ,  $Z_m Z_P/Z_A$  and  $Z_m Z_S/Z_V$  [20].

The difficulty in extending this to larger lattice spacings is the occurrence of exceptional configurations. These can be regulated by taking  $m_q \neq 0$ , and the SCRI group finds that the mass dependence of  $c_{\text{SW}}$  is very weak, so that for  $\beta \geq 5.7$  [21],

$$c_{\text{SW}} = \frac{1 - 0.6084 g^2 - 0.2015 g^4 + 0.03075 g^6}{1 - 0.8743 g^2} \quad (15)$$

within 1% of the Alpha curve for  $\beta \geq 6.0$ . At fixed quark mass, defined by  $m_V/m_{\text{PS}} = 0.7$ , at  $\beta = 5.7$ , scaling violations are reduced from 41% to 3% in  $m_V$ , and from 33% to 2% in  $m_N$  [21].

A comparison of the scaling violations in the vector meson mass, at the same fixed quark mass, for various  $O(a)$ -improved actions is given in Fig 9. Consistent continuum extrapolations, linear in  $a^2$ , are possible for the non-perturbatively improved results, in agreement with  $O(a)$  extrapolation of the Wilson data, but, if the tadpole-improved results are also to be consistent, their continuum extrapolation must include a term linear in  $a$  [22]. Also, it is interesting that the staggered results show big  $O(a^2)$  scaling violations. The QCDSF Collaboration now has results for the non-perturbatively  $O(a)$ -improved Wilson action at a smaller lattice spacing ( $\beta = 6.4$ ) than in Fig 9, which confirm the smooth approach to the continuum limit [23].

The Alpha Collaboration has computed the clover coefficient for non-perturbative  $O(a)$ -improvement of two-flavour QCD with Wilson quarks, obtaining

$$c_{\text{SW}} = \frac{1 - 0.454 g^2 - 0.175 g^4 + 0.012 g^6 + 0.045 g^8}{1 - 0.720 g^2} \quad (16)$$

valid for  $\beta \geq 5.4$  and probably for  $\beta \geq 5.2$  [24].

##### 4.2. Improved staggered quark actions

The motivation for improving staggered quark actions is rather different from that for Wilson quarks. The main objective is to reduce flavour symmetry breaking by reducing the coupling of

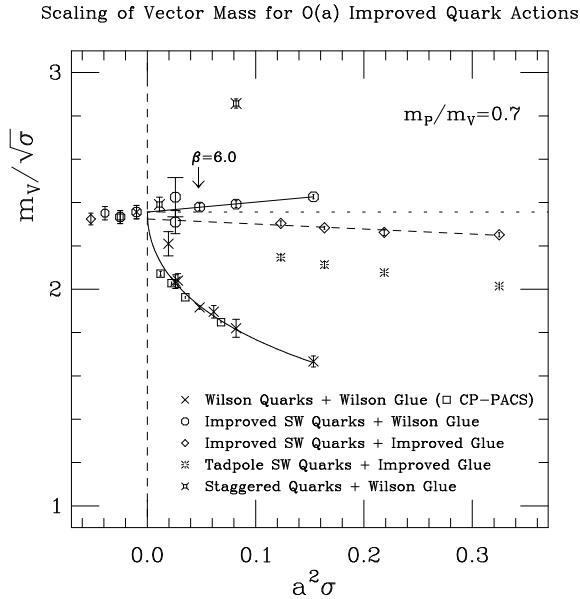


Figure 9. Comparison of scaling violations in the vector meson mass, computed in quenched QCD using the standard Wilson action and several different  $O(a)$ -improved actions [22].

quarks to high-momentum gluons. These can couple quarks at opposite corners of the Brillouin zone, which correspond to different flavours in the continuum. Unfortunately, there are 15 dimension-6 terms which can contribute to the action at  $O(a^2)$ , making a non-perturbative estimate of their coefficients almost impossible [25]. One-loop perturbation theory is typically unreliable for staggered quarks, and so the only practical option is to use tadpole estimates.

MILC has investigated the Naik quark action, in which a three-link hopping term is used to cancel  $O(a^2)$  terms in the staggered-quark action at tree level, and then the coefficients are tadpole-improved [26]. The gluon action they use is  $O(a^2)$  one-loop tadpole improved. Results are compared with those from staggered quarks using both the standard, and the improved gluon action. The observed scaling violations are  $O(a^2)$  and are minimised primarily by the use of improved glue at low quark mass, and by the use of the Naik action

at large quark mass. The speed of light from the continuum dispersion relation is closer to unity for the Naik action than for the staggered action (both with improved glue), whereas flavour breaking, measured from the splitting between the non-Goldstone and the Goldstone pions, is most sensitive to the use of improved glue, in line with the above intuition and previous results using ‘fat’ (ie APE smeared) links [27].

Lagaë and Sinclair have generalised the MILC fat-link action, achieving a similar reduction in flavour violation [28]. For dynamical staggered quarks, MILC also finds that improving the gauge action or fattening the links improves the flavour symmetry [29].

Fat links can be used with the SW action to allow  $c_{SW}$  to be tuned to minimise the spread of near-zero modes [30]. The smeared links allow a small enough value of  $c_{SW}$  to avoid exceptional configurations and, being less sensitive to UV modes of the gauge fields, renormalisation constants are closer to 1 than for the standard SW action.

#### 4.3. Higher-order improvement

The most adventurous improved action hunters seek small scaling violations on very coarse lattices. Inspired by the fixed-point action, DeGrand has been testing fermion actions which couple all the fields on a  $3^4$  hypercube [31]. He finds rotational invariance (ie the speed of light from the continuum dispersion relation is close to 1) even at  $a = 0.36$  fm, although more complicated Pauli interactions seem no better than the simple clover term, Eq (13), for boosting the hyperfine splitting.

The  $O(a^3)$ -accurate D234c quark action of Alford et al. [32], with plaquette plus  $2 \times 1$  rectangle gluon action and mean-link (Landau gauge) tadpole-improved coefficients, has scaling violations of only 7% (in  $m_\phi$  at  $m_{PS}/m_V = 0.7$ ), and a much better dispersion relation than the SW action, at a lattice spacing as large as 0.4 fm.

Thus, while non-perturbative  $O(a)$  improvement for Wilson quarks is well-established for quenched QCD, and so sets almost a mandatory minimum improvement level for dynamical simulations, there are further encouraging signs that



the big gains from higher-order improved actions could become a practical reality.

## 5. NON-PERTURBATIVE QUARK MASS RENORMALISATION

Most of the existing results for quark masses have used perturbative matching and continuum extrapolation. There are some indications that this procedure may not be fully under control. Inconsistencies between the results from using different definitions and different actions cast doubt on the use of perturbation theory, but the issue may be clouded by discretisation errors. Consequently, the main progress this year has not been to increase the precision of the mass estimates compared to last year's review [33], but rather in implementing two non-perturbative matching schemes. The work described below is entirely in the quenched approximation.

### 5.1. Perturbative matching

The CP-PACS results, given in Eqs (8) and (9), obtained with the Wilson action and 1-loop  $Z$  factors, may be compared with the QCDSF group's new results using the non-perturbative  $O(a)$ -improved Wilson action [23].

QCDSF has new data at  $\beta = 6.2$  (on  $24^3 \times 48$  and  $32^3 \times 64$  lattices) and at  $\beta = 6.4$  (on a  $32^3 \times 48$  lattice). They determine the quark masses using the axial Ward identity, with non-perturbative values of  $Z_A$  from the Alpha Collaboration, and tadpole-improved 1-loop perturbative values for  $Z_P$  in Eq (7). They fix the strange quark mass from  $M_K$  and extrapolate results at  $\beta = 6.0, 6.2$  and  $6.4$  linearly in  $a^2$  to the continuum, obtaining

$$m_{ud}^{\overline{\text{MS}}}(2 \text{ GeV}) = 4.13 \pm 0.08 \text{ MeV} \quad (17)$$

$$m_s^{\overline{\text{MS}}}(2 \text{ GeV}) = 98.1 \pm 2.4 \text{ MeV} \quad (18)$$

which are lower than the CP-PACS values, and significantly so for the strange quark.

Working at fixed lattice spacing, with tree-level  $O(a)$ -improved Wilson quarks at the same  $\beta$  values as QCDSF, Giménez et al. [8,34] also find that the strange quark mass defined by the axial Ward identity with perturbative matching is significantly lower than that from the vector Ward identity, or from the non-perturbative RI scheme

(see below). However, the difference could partly be due to discretisation effects.

Before discussing non-perturbative matching, it is interesting to note that the first results for quark masses using domain wall fermions were reported this year [35]. The preliminary results, using  $M_K$  to fix the strange quark mass,  $f_\pi$  to set the scale, and perturbative matching, at  $\beta = 5.85, 6.0$  and  $6.3$ , appear to scale within relatively large errors. The weighted average is  $m_s^{\overline{\text{MS}}}(2 \text{ GeV}) = 82(15) \text{ MeV}$ . While the error is too large to add much new information at the moment, the result shows that domain wall fermions can provide a valuable independent determination of quark masses.

### 5.2. The non-perturbative RI scheme

In the RI scheme [36,8], renormalisation conditions are imposed on amputated Green functions between quark states of momentum  $p$  in Landau gauge, setting them equal to their tree-level values and thereby maintaining Ward identities. Eg for  $O_\Gamma = \overline{q}\Gamma q$ , the amputated Green function is

$$\Lambda_O(pa) = S_q(pa)^{-1} G_O(pa) S_q(pa)^{-1} \quad (19)$$

where the Green function,  $G_O(pa)$ , and quark propagator,  $S_q(pa)$ , are computed by Monte Carlo. Then the renormalisation condition is

$$Z_O^{\text{RI}}(\mu a) Z_q^{-1}(\mu a) \text{Tr } P_O \Lambda_O(pa) \Big|_{p^2=\mu^2} = 1, \quad (20)$$

where  $P_O$  projects onto the tree-level amputated Green function and  $Z_q$  is the wavefunction renormalisation constant. In this way, gauge-dependent non-perturbative renormalisation is achieved at the lattice scale  $\mu \simeq a^{-1} \simeq 2-4 \text{ GeV}$ .

In order to obtain results in the  $\overline{\text{MS}}$  scheme, a continuum perturbative matching calculation is required. This has now been done at next-to-next-to-leading order (NNLO) [37], ie to  $O(\alpha_s^2)$ , and, when combined with the non-perturbative RI result, cancels the gauge dependence.

As mentioned above, this method has been applied to tree-level  $O(a)$ -improved Wilson quarks at  $\beta = 6.0, 6.2$  and  $6.4$ , using both the vector and axial Ward identity definitions of quark mass [8, 34]. These definitions give consistent results in the non-perturbative RI scheme, and show no lattice-spacing dependence over the range studied

(although they are not consistent with the results of perturbative matching), so the best estimates, obtained by averaging the data, are [34]

$$m_{ud}^{\overline{\text{MS}}}(2 \text{ GeV}) = 5.7 \pm 0.5 \pm 0.8 \pm 0.8 \text{ MeV} \quad (21)$$

$$m_s^{\overline{\text{MS}}}(2 \text{ GeV}) = 130 \pm 8 \pm 15 \pm 15 \text{ MeV} \quad (22)$$

where the errors are due to statistics, non-perturbative renormalisation and systematics, respectively. Clearly, the errors in these estimates are too large at present to resolve the discrepancy between Eq (18) (QCDSF) and Eq (8) (CP-PACS).

Kilcup and Pekurovsky [38] have reported preliminary results for the strange quark mass obtained using non-perturbative RI renormalisation for staggered quarks, extrapolated to the continuum from data at  $\beta = 6.0, 6.2$  and  $6.4$ . They obtain  $m_s^{\overline{\text{MS}}}(2 \text{ GeV}) = 129 \pm 23 \text{ MeV}$ , in good agreement with other estimates.

What is needed now is a higher statistics determination, using an improved action ( $O(a)$ -improved Wilson, or staggered), which allows for a reasonably confident continuum extrapolation to compare with the CP-PACS and QCDSF perturbatively-matched results.

### 5.3. Non-perturbative running of the quark mass

As reported last year [39], the Alpha Collaboration has been implementing a non-perturbative method for running the quark mass in the Schrödinger Functional (SF) scheme from low to high scales. The  $O(a)$ -improved PCAC mass in the SF scheme is [40]

$$\overline{m}_{\text{SF}}(2L) = \frac{Z_A(1 + b_A am_q)}{Z_P(2L)(1 + b_P am_q)} m_{\text{lat}}^{\text{PCAC}} \quad (23)$$

where  $m_{\text{lat}}^{\text{PCAC}}$  is defined by the ratio of matrix elements in Eq (7), in which the axial vector current and pseudoscalar density are improved to order  $a$ , as in Eq (14). Here the scale dependence comes through  $Z_P(2L)$ , which is defined in the SF scheme in a box of linear size  $2L$ .

Non-perturbative running is implemented via step scaling functions,

$$\overline{g}_{\text{SF}}^2(2L) = \sigma(2, \overline{g}_{\text{SF}}^2(L)) \quad (24)$$

$$Z_P(2L) = \sigma_P(2, \overline{g}_{\text{SF}}^2(L)) Z_P(L), \quad (25)$$

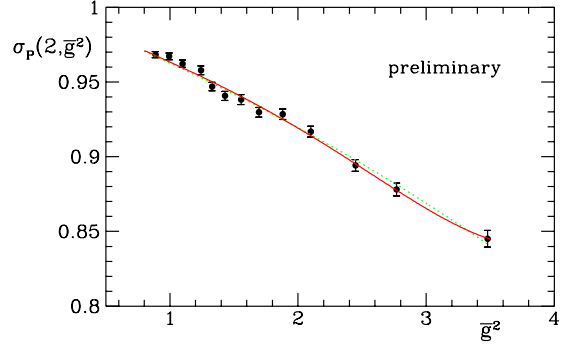


Figure 10. Step scaling function for the quark mass in quenched QCD [40].

which can be iterated to generate a sequence of couplings and quark masses,

$$\begin{aligned} u_k &= \overline{g}_{\text{SF}}^2(2^k L), & m_k &= \overline{m}_{\text{SF}}(2^k L) \\ u_{k+1} &= \sigma(2, u_k), & m_{k+1} &= m_k / \sigma_P(2, u_k). \end{aligned} \quad (26)$$

The step scaling functions are computed for different lattice spacings and extrapolated to the continuum limit. The step scaling function for the quark mass is shown in Fig 10.

Successive application of  $\sigma_P$  yields ratios

$$\begin{aligned} \frac{\overline{m}_{\text{SF}}(L_{\text{max}})}{\overline{m}_{\text{SF}}(2L_{\text{max}})}, \frac{\overline{m}_{\text{SF}}(L_{\text{max}}/2)}{\overline{m}_{\text{SF}}(2L_{\text{max}})}, \dots \\ \dots, \frac{\overline{m}_{\text{SF}}(L_{\text{max}}/2^8)}{\overline{m}_{\text{SF}}(2L_{\text{max}})}. \end{aligned} \quad (27)$$

At the smallest coupling, the SF quark mass can be related to the RG invariant mass, Eq (1), through

$$\frac{\overline{m}}{M} = (2b_0 \overline{g}^2)^{d_0/2b_0} \exp \int_0^{\overline{g}} dg \left[ \frac{\tau(g)}{\beta(g)} - \frac{d_0}{b_0 g} \right] \quad (28)$$

and, hence, the evolution of the running quark mass between this high-energy scale and the original low-energy scale,  $2L_{\text{max}}$ , is determined. This universal result is shown in Fig 11.

At the lowest energy, Alpha obtains

$$2L_{\text{max}} = 1.436 r_0 \simeq 0.72 \text{ fm} \quad (29)$$

$$\frac{M}{\overline{m}_{\text{SF}}(2L_{\text{max}})} = 1.166 \pm 0.015 \pm 0.008. \quad (30)$$

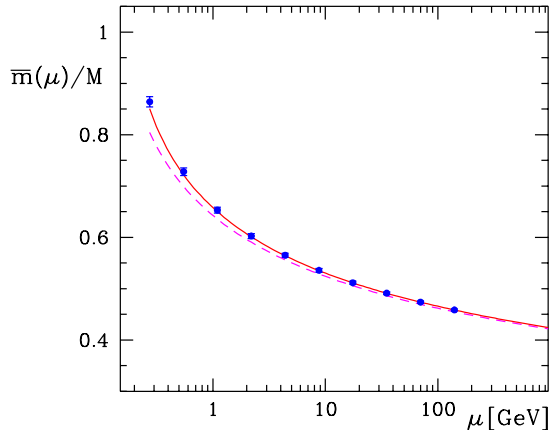


Figure 11. Universal running of the SF quark mass in quenched QCD [40].

So the total renormalisation factor is

$$\frac{M}{m_{\text{lat}}} = 1.166(17) \frac{Z_A(g_0)(1 + b_A a m_q)}{Z_P(g_0, 2L_{\text{max}})(1 + b_P a m_q)} \quad (31)$$

where  $b_A - b_P$  is small enough to be safely neglected [20]. The matching to the lattice scheme is completed by computing  $Z_P(g_0, 2L_{\text{max}} = 1.436r_0)$  for a range of  $\beta$  values, by finding  $(\beta, L/a)$  so that  $L/a = 1.436r_0/a$ , using known values of  $r_0/a$  [41]. The results are shown in Fig 12, where the two sets of results correspond to using the 1- and 2-loop estimates for the boundary counterterm,  $c_t$ , which is only known perturbatively. All that is required now, for example, is the PCAC mass,  $(m_u + m_s)_{\text{lat}}$ , from a standard simulation, to obtain the RG invariant mass  $M_u + M_s$ . Currently, this last step is missing, but suitable data have been generated by both QCDSF and UKQCD.

## 6. GLUEBALLS & HYBRIDS

Finally, I will turn to phenomenology. Quenched QCD predictions are playing an important part in glueball and hybrid meson searches [42]. The challenge is to quantify mixing and sea-quark effects.

### 6.1. The lightest glueball

Lee and Weingarten [43] have estimated the mixing of the lightest discrete isosinglet states.

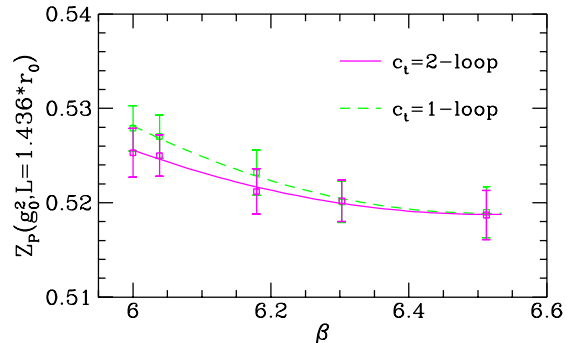


Figure 12. Renormalisation factor for the pseudoscalar density in the SF scheme at the low-energy scale  $2L_{\text{max}}$ , as a function of the gauge coupling in quenched QCD [40].

Their results for the unmixed scalar quarkonium mass are shown in Fig 13, together with their best estimate of the  $O^{++}$  glueball mass, from world data. From the relative ordering of the continuum glueball and  $s\bar{s}$  meson, it is plausible that the  $f_0(1710)$  is predominantly glue. Lee and Weingarten have computed the mixing energy, and use it to fit the experimental data to a crude model of the mixing between the glueball, and the scalar  $s\bar{s}$  and  $(u\bar{u} + d\bar{d})/\sqrt{2}$  (which they denote  $n\bar{n}$ ) states, with the result

$$|f_0(1710)\rangle = 0.86(5)|g\rangle + 0.30(5)|s\bar{s}\rangle + 0.41(9)|n\bar{n}\rangle \quad (32)$$

$$|f_0(1500)\rangle = -0.13(5)|g\rangle + 0.91(4)|s\bar{s}\rangle - 0.40(11)|n\bar{n}\rangle \quad (33)$$

$$|f_0(1390)\rangle = -0.50(12)|g\rangle + 0.29(9)|s\bar{s}\rangle + 0.82(9)|n\bar{n}\rangle, \quad (34)$$

which points to the  $f_0(1710)$  being 74% glueball. They argue that, despite being largely  $s\bar{s}$ , the opposite sign of  $|s\bar{s}\rangle$  and  $|n\bar{n}\rangle$  in  $|f_0(1500)\rangle$  suppresses its decay to  $K\bar{K}$ , in line with the experimental observation.

### 6.2. Hybrid mesons

The UKQCD quenched QCD result [44] that the lightest  $s\bar{s}$  exotic meson has  $J^{PC} = 1^{-+}$  and a mass of 2.0(2) GeV, is supported by further quenched results reported by MILC this year [45]. SESAM has repeated the UKQCD analysis using

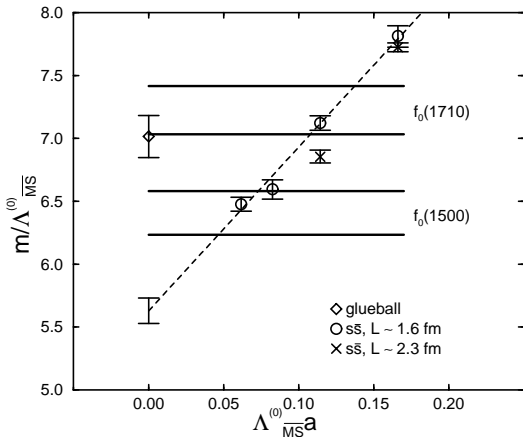


Figure 13. Continuum extrapolation of the unmixed scalar  $s\bar{s}$  mass, compared with the continuum limit of the scalar glueball in quenched QCD and the masses of the  $f_0(1710)$  and the  $f_0(1500)$  (the error bands are due to the uncertainty in  $\Lambda_{\overline{\text{MS}}}^{(0)}$ ) [43].

Wilson  $N_f = 2$  configurations at  $\beta = 5.6$ . They are able to perform a linear chiral extrapolation in the dynamical quark mass, from data at four quark masses, and find that the  $1^{-+}$  remains the lightest exotic, with a mass of 1.9(2) GeV, which is consistent with the quenched results [46]. Of course, exotic mesons are expected to mix with four-quark states. This mixing is currently under investigation by SESAM.

For the wider particle physics community, predictions for glueballs and hybrid mesons (along with the light quark masses) are the most interesting output of our light hadron work, and pursuing a more systematic analysis of mixing and sea-quark effects will be an important part of our future programme.

## 7. CONCLUSIONS & ACKNOWLEDGEMENTS

In summary, we now have precise results from CP-PACS which indicate that quenched QCD fails to reproduce the light hadron spectrum at the few percent level. Even so, there may be lin-

gering doubts about the reliability of the continuum extrapolation, as there is no confirmation yet from improved actions. For quark masses, we are on the verge of resolving discrepancies between different simulations, which are probably due to the unreliability of perturbative matching. Techniques for non-perturbative renormalisation are well-developed and should be mandatory from now on. It is time for a definitive simulation of quenched QCD using non-perturbative  $O(a)$ -improved Wilson, or staggered quarks and non-perturbative matching, to establish the quenched light hadron spectrum and quark masses once and for all.

Simulations with two flavours of dynamical quarks are showing hints that the strange hadron spectrum is in better agreement with experiment than in quenched QCD, although the quenched approximation must still be used for the strange quark. The biggest effect observed so far is that the light quark masses are around 40% smaller than in quenched QCD. String breaking has not been seen yet, but it should be within reach of present day simulations, and there is much to be done to improve our understanding of mixing and sea-quark effects on glueball and hybrid states.

Somewhat surprisingly, quenched QCD has turned out to be a rather accurate effective theory for many quantities. Knowing its limitations should give us greater confidence in using it as a phenomenological model for quantities where 10-20% accuracy is useful. To improve on it, will require simulations with several different combinations of sea-quark flavours, in order to be able reliably to interpolate/extrapolate to the flavour content of the real world. We have reached the point where quenched QCD can be simulated with sufficient accuracy and this gives us a solid foundation from which to tackle the flavour dependence of QCD.

I wish to thank M. Alford, R. Burkhalter, L. Giusti, M. Golterman, S. Gottlieb, S. Güsken, T. Klassen, P. Lacock, K.-F. Liu, X.-Q. Luo, T. Mendes, C. McNeile, T. Okude, S. Ohta, E. Pallante, G. Schierholz, D. Sinclair, A. Soni, A. Vladikas, D. Weingarten, M. Wingate, H. Wittig, and T. Yoshié for sending me their results in advance.

## REFERENCES

1. A.J. Buras et al., Phys. Lett. 389B (1996) 749.
2. T. Yoshié, Nucl. Phys. B (Proc. Suppl.) 63A-C (1998) 3.
3. R. Burkhalter, these proceedings.
4. T. Yoshié, these proceedings.
5. A. Morel, J. Physique 48 (1987) 111; S.R. Sharpe, Phys. Rev. D41 (1990) 3233, D46 (1992) 3146; C.W. Bernard and M.F.L. Golterman, ibid D46 (1992) 853.
6. G. Colangelo and E. Pallante, hep-lat/9708005.
7. S.R. Sharpe, hep-lat/9707018; M.F.L. Golterman and K.C. Leung, hep-lat/9711033.
8. V. Giménez et al., hep-lat/9801028.
9. C. Bernard et al., hep-lat/9805004.
10. S. Gottlieb, these proceedings.
11. S. Kim, these proceedings.
12. N. Eicker et al., hep-lat/9806027.
13. K. Kanaya, these proceedings.
14. M. Talevi, these proceedings.
15. N. Eicker et al., Phys. Lett. B407 (1997) 290.
16. H. Leutwyler, hep-ph/9609467.
17. O. Philipsen, these proceedings.
18. J. Kuti, these proceedings.
19. M. Lüscher, hep-lat/9802029.
20. G.M. De Divitiis and R. Petronzio, hep-lat/9710071.
21. R.G. Edwards et al., hep-lat/9711052.
22. T.R. Klassen, these proceedings.
23. D. Pleiter, these proceedings.
24. K. Jansen and R. Sommer, hep-lat/9803017.
25. Y. Luo, Nucl. Phys. B (Proc. Suppl.) 63A-C (1998) 889.
26. C. Bernard et al., hep-lat/9712010.
27. T. Blum et al., Phys. Rev. D55 (1997) 1133.
28. J.-F. Lagaë and D.K. Sinclair, hep-lat/9806014.
29. D. Toussaint, these proceedings; K. Orginos and D. Toussaint, hep-lat/9805009.
30. T. DeGrand, these proceedings; T. DeGrand et al., hep-lat/9807002.
31. T. DeGrand, these proceedings and hep-lat/9802012.
32. M. Alford et al., hep-lat/9712005.
33. T. Bhattacharya and R. Gupta, Nucl. Phys. B (Proc. Suppl.) 63A-C (1998) 95.
34. L. Giusti, these proceedings.
35. M. Wingate, these proceedings.
36. G. Martinelli et al., Nucl. Phys. B445 (1995) 81.
37. E. Franco and V. Lubicz, hep-ph/9803491.
38. D. Pekurovsky, these proceedings.
39. S. Capitani et al., Nucl. Phys. B (Proc. Suppl.) 63A-C (1998) 153.
40. H. Wittig, these proceedings.
41. M. Guagnelli, hep-lat/9806005; R. Sommer, these proceedings.
42. F.E. Close, Nucl. Phys. B (Proc. Suppl.) 63A-C (1998) 28.
43. W. Lee and D. Weingarten, hep-lat/9805029; D. Weingarten, these proceedings.
44. P. Lacock et al., Phys. Lett. B401 (1997) 308.
45. C. McNeile, these proceedings.
46. P. Lacock, these proceedings.